Chapter 1:

Efficient Interaction Between Two GTPases Allows the Chloroplast SRP Pathway to Bypass the Requirement for an SRP RNA

A version of this chapter has been published as:

Jaru-Ampornpan, P., Chandrasekar, S., and Shan, S. (2007) *Mol. Biol. Cell*, **18** (7), 2636–2545.

Abstract

Co-translational protein targeting to membranes is regulated by two GTPases in the signal recognition particle (SRP) and the SRP receptor (SR); association between the two GTPases is slow and is accelerated 400-fold by the SRP RNA. Intriguingly, the otherwise universally conserved SRP RNA is missing in a novel chloroplast SRP pathway. We found that even in the absence of an SRP RNA, the chloroplast SRP and SR can interact efficiently with one another; the kinetics of interaction between the chloroplast GTPases is 400-fold faster than their bacterial homologues and matches the rate at which the bacterial SRP and SR interact with the help of SRP RNA. Biochemical analyses further suggest that the chloroplast FtsY is pre-organized in a conformation that allows optimal interaction with its binding partner, so that conformational changes during complex formation are minimized. Our results highlight intriguing differences between the classical and chloroplast SRP and SR GTPases, and help explain how the chloroplast SRP pathway can mediate efficient targeting of proteins to the thylakoid membrane in the absence of the SRP RNA, which plays an indispensable role in all the other SRP pathways.

Introduction

SRP and SR comprise the major cellular machinery that delivers nascent proteins to the eukaryotic endoplasmic reticulum membrane or the bacterial plasma membrane (*1, 2*). The functional core of SRP is the SRP54 protein (called Ffh in bacteria) in complex with an SRP RNA, which recognizes the cargo protein and interacts with the SR (called FtsY in bacteria). The protein targeting reaction is regulated by the guanosine-5'-triphosphate (GTP)-binding domains in both SRP54 and SR. SRP recognizes the signal sequence on nascent polypeptides that emerge from a translating ribosome (*3*). The ribosome•nascent chain complex is delivered to the membrane via the interaction of SRP with SR when both proteins are bound with GTP (*4, 5*). Upon arrival at the membrane, SRP releases the cargo protein to a protein conducting channel embedded in the membrane (*6, 7*), where the nascent protein is either integrated into the membrane or translocated across the membrane to enter the secretory pathway. GTP hydrolysis is stimulated in the SRP•SR complex, which then drives disassembly and recycling of SRP and SR (*8*).

The SRP and SR GTPases comprise a unique subgroup in the GTPase superfamily (*1*). Both proteins have a GTPase, "G" domain that shares homology with the classical *Ras* GTPase fold (*9, 10*). In addition, the SRP-type GTPases contain an N-terminal four-helix bundle, the "N"-domain, that packs tightly against the G domain. The G- and N-domains form a structural and functional unit called the NG domain. Unlike classical signaling GTPases that undergo large conformational changes depending on whether GTP or guanosine 5-diphosphate (GDP) is bound, the structures of these GTPases are similar regardless of which nucleotide is bound (*10, 11*). Substantial

conformational changes occur only when the two GTPases form a complex with one another (*12, 13*). Most notably, the G- and N-domains readjust their relative positions such that the N-domains of both proteins move closer to the dimer interface and form additional interface contacts to stabilize the complex.

The importance of this N-G domain rearrangement is supported by biochemical analyses. Many mutations at this interface disrupt SRP–SR complex formation and protein targeting (*14*). Interestingly, unlike classical GTPases, free FtsY displays little discrimination between GTP and non-cognate nucleotides. In contrast, FtsY acquires substantial nucleotide specificity only when it binds SRP. These results have led to the proposal that during complex formation, FtsY changes from a non-discriminative, "open" state to a "closed" state in which specific interactions between GTP and active site residues are established (*15*). Consistent with these observations, the crystal structure showed that, upon complex formation, the rearrangement at the N-G domain interface brings the nucleotide specificity determinant, Asp449, closer to the bound GTP and within hydrogen bonding distance with the amino group of the guanine ring (*12*). Thus, the N-G domain rearrangement is primarily responsible for the open → closed conformational change that occurs during SRP–SR complex formation and precisely aligns active site residues with respect to the bound GTP.

The unique structural features of the SRP subgroup of GTPases confer upon them many characteristics that are distinct from canonical GTPases. Most importantly, SRP-type GTPases bind nucleotides much more weakly than signaling GTPases and release nucleotides quickly (*16–19*). Therefore, they do not employ nucleotide exchange factors to facilitate the conversion from the GDP- to the GTP-bound form. These GTPases also

do not utilize external GTPase-activating proteins; instead, SRP and SR reciprocally activate one another upon complex formation (*20*).

A third unique feature of the GTPases engaged in the SRP pathway is the requirement for a universally conserved SRP RNA. Mammalian SRP is a cytosolic ribonucleoprotein complex that consists of 6 polypeptides and a 7S SRP RNA molecule. Besides SRP54, the other protein components are not conserved, whereas the SRP RNA has been shown to play an indispensable role in protein targeting in all three kingdoms of life. In early biochemical studies on the mammalian SRP, the SRP RNA appeared to be nothing more than a scaffold that holds all the SRP proteins together in a complex (*21, 22*). The finding that bacteria contain a much simpler SRP, comprised solely of a complex of Ffh and the 4.5S SRP RNA, was therefore intriguing. This smaller RNA contains the most phyllogenetically conserved region of the SRP RNA, domain IV, which is likely to have been maintained for functional purposes (*23, 24*). Subsequently, kinetic analyses of the role of the 4.5S SRP RNA on the GTPase cycles of Ffh and FtsY showed that a major role of this RNA is to accelerate complex formation between the two GTPases. In the absence of the SRP RNA, Ffh–FtsY association is extremely slow, with a rate constant of 5×10^3 $M^{-1}s^{-1}$. The SRP RNA accelerates their association kinetics by 400-fold, to a rate that can allow the SRP and SRP receptor to adequately carry out their biological functions, thus accounting for the indispensable role of the SRP RNA in the bacterial, archeal, and eukaryotic SRP pathways.

A novel SRP targeting pathway was discovered in the chloroplast (*25*). cpSRP54 and cpFtsY are the chloroplast homologues of SRP and SR GTPases, respectively (*26–28*). cpSRP54 recognizes its cargo, the light-harvesting chlorophyll-binding proteins, via

a protein adaptor cpSRP43 (*29*). Together, cpSRP54 and cpSRP43 deliver the cargo protein from the stroma to the thylakoid membrane via the GTP-dependent interaction between cpSRP54 and cpFtsY (*28*). Surprisingly, the otherwise universally conserved SRP RNA has not been found to date in the chloroplast SRP system. To rationalize the absence of the SRP RNA, we characterized the kinetic and thermodynamic features of the GTPase cycles of cpSRP54 and cpFtsY. We found that, unlike their bacterial and mammalian homologues, the chloroplast SRP and SR GTPases can efficiently interact with one another by themselves. This helps explain why the cpSRP pathway could bypass the requirement for an SRP RNA.

Materials and Methods

Protein expression and purification. cpSRP54 from *A. thaliana* was expressed from baculovirus at the Protein Expression Facility of Caltech. Recombinant cpSRP54 is purified by affinity chromatography using Ni-NTA (Qiagen) and cation exchange over a MonoS column (GE Healthcare) using a linear gradient of 150–600 mM NaCl. cpFtsY from *A. thaliana* was expressed and purified as described (*30*). Two additional chromatographic steps [Superdex 75 and monoQ (GE Healthcare)] were added to remove contaminating GTPases. Mutant cpFtsY(D283N) was constructed using the QuickChange procedure (Stratagene) and was expressed and purified by the same procedure as that for wild-type cpFtsY.

Kinetics. All reactions were carried out at 25 °C in assay buffer [50 mM KHEPES (pH 7.5), 150 mM KOAc, 2mM $Mg(OAc)_2$, 2mM DTT, 0.01% Nikkol]. GTP hydrolysis reactions were followed and analyzed as described (*19*). The general procedures for characterizing the basal and stimulated GTPase reactions between SRP and SR have been described in detail (*15, 19, 31*) and are summarized briefly here. The justification for how each microscopic rate constant was derived from these measurements is provided in Supplementary Material.

Basal GTPase or XTPase activities of cpSRP54, cpFtsY, and cpFtsY(D283N) were measured in single-turnover reactions as described ([GTP] << [E]; (*19*)). The dependence of the observed rate constant (k_{obsd}) on protein concentration were fit to eq 1, in which k_{max} is the maximal rate constant at saturating protein concentrations, and $K_{1/2}$ is the protein concentration required to reach half the maximal rate.

$$k_{obsd} = k_{\max} \times \frac{[\text{protein}]}{K_{1/2} + [\text{protein}]} \quad \textbf{(1)}$$

The nucleotide affinities of the GTPases were determined using several independent methods. The GTP affinities for cpSRP54 and cpFtsY and the XTP (xanthosine-5'-triphosphate) affinity for cpFtsY(D283N) were obtained from the $K_{1/2}$ values obtained in the fits of the basal GTPase or XTPase reactions to eq 1. Because the chemical step is rate-limiting for the basal GTPase and XTPase reactions, $K_{1/2}$ is equal to K_d, the dissociation constant of the nucleotide. The affinities of GDP, GppNHp (5'-guanylylimido-diphosphate), XDP (xanthosine-5'-diphosphate) and XppNHp (5'-xanthylylimido-diphosphate**)** were determined using these nucleotides as inhibitors of the basal GTPase or XTPase reactions (*19*). With sub-saturating protein, the inhibition constant K_i is equal to K_d. Finally, the binding of nucleotides to the GTPases was determined directly by using fluorescent N-methyl-anthraniloyl (mant) derivatives of GTP, GDP, and XTP, as described below.

The reciprocally stimulated GTPase reaction between cpSRP54 and cpFtsY was determined in multiple turnover reactions ([GTP] >> [E]) in the presence of a small, fixed amount of cpSRP54 and varying concentrations of cpFtsY, using a GTP concentration that saturates both GTPase sites. The concentration dependence of the observed rate constant (k_{obsd}) is fit to eq 2, in which k_{cat} is the rate constant at saturating cpFtsY concentrations, and K_m is the

$$k_{obsd} = k_{cat} \times \frac{[\text{cpFtsY}]}{K_m + [\text{cpFtsY}]} \quad \textbf{(2)}$$

concentration of cpFtsY that gives half the maximal rate. The stimulated GTPase reaction between cpSRP54 and GTP-bound cpFtsY(D283N) was determined using the same experimental setup. The stimulated GTPase reaction of cpSRP54 by XTP-bound cpFtsY(D283N) was determined analogously, except that the concentration of GTP and XTP were adjusted such that cpSRP54 was predominantly occupied by GTP whereas cpFtsY(D283N) was predominantly occupied by XTP.

The cpFtsY(D283N)-stimulated GTP hydrolysis from cpSRP54 was also determined in single turnover experiments. The hydrolysis of trace GTP* was monitored in the presence of sub-saturating cpSRP54 and varying amounts of cpFtsY(D283N), with 25 μM XTP present to selectively occupy the active site of cpFtsY(D283N). Under these conditions, the third-order reaction: GTP* + cpSRP54 + cpFtsY(D283N) $^{\bullet XTP}$ → products was followed. The reciprocal reaction, XTP* + cpFtsY(D283N) + cpSRP54$^{\bullet GTP}$ → products was determined using an analogous setup, except that the concentration of cpSRP54 was varied and 25 μM GTP was present to selectively occupy the active site of cpSRP54. The data were fit to eq 1 above. Finally, first-order rate constants of the stimulated GTP and XTP hydrolysis reactions from the $^{*GTP\bullet}$cpSRP54•cpFtsY(D283N)$^{\bullet XTP*}$ complex were determined using high concentrations of both proteins (20–80 μM) in the presence of stoichiometric amounts of their respective nucleotides. The reaction time courses were monitored in a Kintek quench flow apparatus and fit to a single-exponential rate equation to obtain the first-order rate constants.

The effect of XTP on the reaction $^{*GTP\bullet}$cpSRP54 + cpFtsY(D283N)$^{\bullet GTP*}$ → products was determined in the presence of sub-saturating concentrations of both proteins

and a high concentration of GTP (200 μM) to saturate both active sites. The XTP concentration dependence was fit to eq 3, in which k_0 is the rate constant in the absence of any inhibitor, k_1 is the rate

$$k_{obsd} = k_0 \times \frac{K_i^{app}}{K_i^{app} + [\mathrm{XTP}]} + k_1 \times \frac{[\mathrm{XTP}]}{[\mathrm{XTP}] + K_i^{app}} \quad \textbf{(3)}$$

constant at infinite XTP concentrations, and K_i^{app} is the apparent inhibition constant of XTP determined from this experiment. K_i^{app} is related to the dissociation constant of XTP by eq 4,

$$K_i^{app} = K_d^{XTP} \times \left(1 + \frac{[\mathrm{GTP}]}{K_d^{GTP}}\right) \quad \textbf{(4)}$$

in which K_d^{XTP} and K_d^{GTP} are the dissociation constants of XTP and GTP for cpFtsY(D283N), respectively.

Fluorescence. All fluorescence measurements were conducted at 25 °C using the single-photon–counting Fluorolog 3-22 spectrofluorometer (Jobin Yvon). Fluorescence emission spectra of mant-derivatives of GTP, GDP, and XTP were acquired using an excitation wavelength of 356 nm. Nucleotide binding affinities were determined by recording the change in fluorescence intensity at 445 nm in the presence of 0.4–1 μM mant-nucleotides and increasing concentrations of cpSRP54, cpFtsY, or cpFtsY(D283N). The data were fit to eq 5,

$$F_{obsd} = \left(F_{\max} - F_0\right) \times \frac{[\mathrm{protein}]}{K_d + [\mathrm{protein}]} \quad \textbf{(5)}$$

in which F_{max} is the fluorescence at saturating protein concentrations, F_0 is the fluorescence in the absence of any protein, and K_d is the dissociation constant of the mant-nucleotide.

The rate constants for dissociation of mant-GTP and mant-GDP were determined using a pulse chase experiment as described (*16*). The time course for decay of fluorescence was followed in a stopped flow apparatus (Applied Photophysics) and fit to single exponential functions to obtain the dissociation rate constants.

Results

To understand why and how the cpSRP pathway bypasses the requirement for an SRP RNA, which plays a critical role in facilitating the interaction between the SRP and SR GTPases in all the other SRP pathways, we characterized the rate and equilibrium of the individual steps in the GTPase cycles of cpSRP54 and cpFtsY and their GTP-dependent interaction with one another (Figure 1.1). Each protein can bind and hydrolyze GTP by itself (steps 1–3 for cpSRP54 and 1'–3' for cpFtsY). cpSRP54 form a stable complex with cpFtsY when both proteins are bound with GTP (step 4). Both GTP molecules are rapidly hydrolyzed from the complex (step 5). GTP hydrolysis destabilizes the complex and drives its dissociation (step 6). The rate and equilibrium constants for each step are summarized in Table 1.1. For simplicity, additional possibilities such as hydrolysis of one of the GTPs followed by complex disassembly are not shown; these possibilities are presented in the Discussion.

Basal GTPase cycles of cpSRP54 and cpFtsY.

We first determined the basal GTPase activities of the individual GTPases. Both proteins hydrolyze GTP slowly, with maximal hydrolysis rates of 0.017 and 0.0045 min^{-1} at saturating protein concentrations for cpSRP54 and cpFtsY, respectively (Figure 1.2). The protein concentration dependence of the hydrolysis rate gives the affinity of each protein for GTP. Both GTPases bind their substrates weakly, with dissociation constants of 2.8 and 2.1 μM for cpSRP54 and cpFtsY, respectively (Figure 1.2). We also determined the affinities of cpSRP54 and cpFtsY for GDP and the non-hydrolyzable GTP analogue GppNHp by using these nucleotides as competitive inhibitors of the basal

GTPase reactions. Both proteins bind GDP and GppNHp weakly, with inhibition constants in the micromolar range (Table 1.2).

We also directly measured the interaction of nucleotides with both GTPases using fluorescent mant-derivatives of GTP and GDP. Binding of both GTPases to mant-GTP or mant-GDP induces a 50–80% increase in fluorescence (Figure 1.3A and 1.3B, respectively). Titration of this fluorescence change as a function of protein concentration gave dissociation constants of 6.5 and 11 μM for binding of mant-GTP and mant-GDP to cpSRP54, respectively, and 1.9 and 3.1 μM for binding of mant-GTP and mant-GDP to cpFtsY, respectively (Figure 1.3C and 1.3D; Table 1.2). For cpFsY, these affinities are the same, within error, as those of unmodified nucleotides determined using the GTPase assay. For cpSRP54, these affinities are only ~ twofold larger than those of unmodified GTP and GDP. Thus, the mant-group does not significantly perturb the binding of nucleotides.

A hallmark of the SRP subgroup of GTPases is the fast rate at which they release and exchange nucleotides. The weak nucleotide binding affinities of cpSRP54 and cpFtsY suggest that this is also the case for the chloroplast SRP GTPases. This was confirmed by directly measuring the dissociation rate constants of mant-GTP and mant-GDP. As expected, both cpSRP54 and cpFtsY release mant-GTP quickly, with dissociation rate constants of 10.4 and 5.4 s^{-1}, respectively (Figure 1.3E and Table 1.1). Similarly, mant-GDP is released quickly by both cpSRP54 and cpFtsY, with dissociation rate constants of 32 and 8.1 s^{-1}, respectively (Figure 1.3F and Table 1.1). Thus, analogous to their bacterial and mammalian homologues, the chloroplast SRP GTPases hydrolyze GTP slowly and can exchange nucleotides quickly, in contrast to classical

signaling GTPases that release nucleotide slowly (on the order of 10^{-3} – 10^{-4} s^{-1}) and require external exchange factors to facilitate nucleotide release.

Interaction between cpSRP54 and cpFtsY is much more efficient than classical SRP systems.

In classical SRP systems, complex formation between the SRP and SR GTPases is very slow and is accelerated 400-fold by the SRP RNA (*19, 32*). Once a complex is formed, SRP and SR stimulate each other's GTPase activity and the rate of this stimulated GTPase reaction within the complex is also accelerated 5–10 fold by the SRP RNA (*19, 32*). As no SRP RNA has been found in the chloroplast SRP system, we asked whether and how efficiently cpSRP54 and cpFtsY can interact with and activate each other in the absence of an SRP RNA.

To this end, we determined the rate of stimulated GTP hydrolysis reaction in the presence of both cpSRP54 and cpFtsY; GTPase activation in the cpSRP54•cpFtsY complex provides a means to monitor complex formation between the two GTPases (*19, 32*). To our surprise, cpSRP54 and cpFtsY interact with each other efficiently even in the absence of an SRP RNA (Figure 1.4, ●). The slope of the initial linear portion of the protein concentration dependence, which represents the rate constant of the reaction: $^{GTP\bullet}$cpSRP54 + cpFtsY$^{\bullet GTP}$ → products (k_{cat}/K_m), is ~ 400-fold faster than that of the corresponding reaction between the *E. coli* GTPases in the absence of the SRP RNA (Figure 1.4, ▲). Indeed, this rate constant matches that of the *E. coli* GTPases in the presence of the 4.5S SRP RNA (Figure 1.4, ▼). The rate constant at saturating protein concentrations, which represents the rate of GTP hydrolysis within the

^{GTP}•cpSRP54•cpFtsY•^{GTP} complex, is also identical between the chloroplast and the *E. coli* GTPases in the presence of the SRP RNA (● vs. ▼), and eightfold faster than that of the *E. coli* GTPases without the RNA bound (▲).

In the *E. coli* SRP system, complex formation is rate-limiting for the reaction: ^{GTP}•SRP + FtsY•^{GTP} → products (both in the presence and absence of SRP RNA) (*19*). Therefore, k_{cat}/K_m is equal to the association rate constant between the two GTPases. If this were also true for the cpSRP54 and cpFtsY, then the association between cpSRP54 and cpFtsY would be 400-fold faster than their *E. coli* homologues. Alternatively, k_{cat}/K_m is limited by the chemical step instead of complex formation for the chloroplast GTPases. If this were true, then the difference in association rates between the chloroplast and *E. coli* GTPases would be even greater. Thus the results in Figure 1.4 demonstrate that complex formation between the chloroplast SRP and SR GTPases is much more efficient than that of their bacterial and mammalian homologues and thus do not need the help from an SRP RNA.

cpFtsY exhibits high nucleotide specificity.

Association between bacterial SRP and SR GTPases is slow presumably because significant domain rearrangements are required to form a stable complex, including a change from the open to the closed conformation that is manifested functionally as an increase in the nucleotide specificity of the *E. coli* FtsY ((*15*); see Introduction). We hypothesized that the chloroplast SRP GTPases are pre-organized in the closed

conformation even in the absence of their binding partner, thus reducing the cost for the open → closed rearrangement and resulting in a faster rate of protein–protein interaction.

A prediction from this model is that cpFtsY can effectively discriminate between cognate and non-cognate nucleotides by itself without the help from cpSRP54. To test this idea, we mutated the conserved specificity determinant, Asp283, to an asparagine. This mutation converts many GTPases to XTP-specific proteins by swapping the hydrogen bond between the carboxylate oxygen of Asp and the exocyclic amino group of the guanine ring (*33–36*). As predicted, wild-type cpFtsY preferentially hydrolyzes GTP. The rate constant of the reaction: GTP* + FtsY → GDP + P_i* is 37-fold faster than that of mutant cpFtsY(D283N) (Figure 1.5A). Similarly, mutant cpFtsY(D283N) hydrolyzes XTP much faster than wild-type cpFtsY (Figure 1.5B). In contrast, *E. coli* FtsY exhibits no more than a fourfold difference between wild-type and mutant GTPases in the hydrolysis rates of either nucleotide (*15*).

We next asked if cpFtsY can specifically bind its cognate nucleotide. Using both the GTPase assays (Figure 1.5C and 1.5D) and fluorescent mant-nucleotides (Figure 1.5E and 1.5F), we showed that wild-type cpFtsY preferentially binds guanine-based nucleotides, with affinities 40–70-fold higher than mutant cpFtsY(D283N) (Table 1.2). Analogously, mutant cpFtsY(D283N) preferentially binds xanthine-based nucleotides, with affinities 90–250-fold higher than wild type cpFtsY (Table 1.2). In contrast, *E. coli* FtsY exhibits no more than a twofold discrimination between wild-type and mutant GTPases for any nucleotides (*15*). Together, the results in this section show that, unlike

its bacterial homologue, the active site of cpFtsY can specifically recognize GTP even in the absence of cpSRP54. This is consistent with the notion that free cpFtsY is already in the closed conformation and pre-organized to interact with cpSRP54.

GTPase activation between cpSRP54 and cpFtsY is reciprocal but asymmetric.

The XTP-specific mutant cpFtsY(D283N) also allowed us to test whether cpSRP54 and cpFtsY reciprocally stimulate the GTPase activity of one another, as is the case for the bacterial system. If this were the case, XTP hydrolysis by cpFtsY(D283N) would be stimulated by cpSRP54 and, conversely, GTP hydrolysis by cpSRP54 would be stimulated by cpFtsY(D283N).

To examine the effect of cpFtsY(D283N) on GTP hydrolysis by cpSRP54, we measured the rate of GTP hydrolysis in the third-order reaction: GTP* + cpSRP54 + $D283N^{\bullet XTP} \rightarrow$ GDP + P_i*. As predicted, the rate of GTP hydrolysis is significantly stimulated by the presence of cpFtsY(D283N) (Figure 1.6A), consistent with the notion that cpFtsY acts as the activating protein for cpSRP54. Analogously, the reciprocal reaction, XTP hydrolysis by cpFtsY(D283N), is significantly stimulated by the presence of cpSRP54 (Figure 1.6B; the third-order reaction: XTP* + D283N + $cpSRP54^{\bullet GTP} \rightarrow$ XDP + P_i* was followed).

Interestingly, the rate of stimulated GTP hydrolysis from cpSRP54 is ~ tenfold slower than that of XTP hydrolysis from cpFtsY(D283N) (see rates in Figure 1.6A and 1.6B), raising the possibility that nucleotide hydrolyses from the two GTPase sites in the complex are *not* symmetric. To test this possibility, we formed the

^{GTP}•cpSRP54•cpFtsY(D283N)•^{XTP} complex by using high concentrations of both proteins and stoichiometric amounts of GTP and XTP, and directly measured the rate constants for hydrolysis of both GTP and XTP from this complex. As shown in Figure 1.6C, the rate constant for XTP hydrolysis is 3.7 min^{-1} (squares), over fourfold faster than the rate constant of 0.87 min^{-1} for GTP hydrolysis (circles). This represents only a lower limit for the difference in hydrolysis rates between the two active sites, because cpFtsY(D283N) bound with GTP is much more active in binding and activating cpSRP54 (see the next section), even though it preferentially binds XTP by itself. Thus, part of the GTP hydrolysis rate observed in Figure 1.6C (circles) is contributed by an alternative ^{GTP}•cpSRP54•cpFtsY(D283N)•^{GTP} complex. The actual difference between the hydrolysis rates from the two active sites is larger than that observed in Figure 1.6C and is closer to the ~ tenfold difference observed in Figures 1.6A and 1.6B, which monitors the third-order reaction rates. Under these conditions, the observed reaction rates are determined by the affinity of free cpSRP54 and cpFtsY(D283N) for their respective nucleotides as well as the rate at which GTP and XTP are hydrolyzed from the respective active sites in the complex. Since cpSRP54 and cpFtsY(D283N) exhibit similar affinities for GTP and XTP, respectively (Table 1.2), the observed ~ tenfold difference in reaction rate (Figures 1.6A and 1.6B) primarily reflects the difference in hydrolysis rate from the two active sites. Thus, like the classical SRP systems, cpSRP54 and cpFtsY act as reciprocal activating proteins for one another, yet unlike their bacterial homologues, nucleotide hydrolyses from the two active sites are asymmetric.

Mutant cpFtsY(D283N) prefers GTP over XTP upon complex formation with cpSRP54.

Another intriguing observation from the results in Figure 1.6C is that the rate constants of the stimulated GTPase and XTPase reactions from the ^{GTP}•cpSRP54•cpFtsY(D283N)•^{XTP} complex (0.87 and 3.7 min^{-1}, respectively) are over tenfold slower than that from the wild-type ^{GTP}•cpSRP54•cpFtsY•^{GTP} complex (Figure 1.4), even accounting for the fact that two GTP molecules are hydrolyzed in the wild-type complex. Therefore, we suspected that the D283N mutation or the replacement of GTP with XTP renders cpFtsY less active in binding and activating cpSRP54. This is reminiscent of the behavior of an XTP-specific mutant of the *E. coli* SRP GTPase, SRP(D251N), which is deficient in binding and activating FtsY in its XTP-bound form. Instead, mutant SRP(D251N) can better bind and activate FtsY when bound to the non-cognate GTP (*31*).

To test whether this is also the case for mutant cpFtsY(D283N), we measured the rate constant for GTP hydrolysis from the ^{GTP}•cpSRP54•cpFtsY(D283N)•^{GTP} complex when cpFtsY(D283N) is forced to bind its non-cognate nucleotide by using a high GTP concentration. When mutant cpFtsY(D283N) is bound with the non-cognate GTP, the rate of stimulated GTP hydrolysis is much faster than when it is bound with the cognate XTP (Figure 1.7A, diamonds vs. squares). The rate constant at saturating protein concentration, which represents the rate constant for GTP hydrolysis from the ^{GTP}•cpSRP54•cpFtsY(D283N)•^{GTP} complex, is comparable to that of the wild-type complex (Figure 1.7A; diamonds vs. circles), suggesting that the

^{GTP}•cpSRP54•cpFtsY(D283N)•^{GTP} complex achieves the same active conformation as the complex formed by the wild-type proteins. As a ~ fivefold higher concentration of mutant cpFtsY(D283N) than wild-type cpFtsY is required to reach saturation, complex formation is modestly compromised for GTP-bound cpFtsY(D283N) (Figure 1.7A; diamonds vs. circles). In contrast, no saturation is observed in the reaction with XTP-bound cpFtsY(D283N) up to 30 μM (squares), indicating that complex formation is significantly compromised when the mutant is bound with its cognate nucleotide. Thus, mutant cpFtsY(D283N) prefers the non-cognate GTP over cognate XTP when it forms a complex with cpSRP54.

To provide independent evidence on this switch in nucleotide preference upon complex formation, we explored the effect of XTP on the rate of the reaction: ^{GTP}•cpSRP54 + cpFtsY(D283N)•^{GTP} → products. If cpFtsY(D283N) is less active in binding and activating the GTPase reaction of cpSRP54 when it is bound with cognate XTP than with non-cognate GTP, then addition of XTP, which competes off the GTP bound at the active site of cpFtsY(D283N), should inhibit the stimulated GTPase reaction. As predicted, addition of XTP inhibits this stimulated reaction (Figure 1.7B). The observed inhibition constant for XTP is 9.0 μM, consistent with the expected value of 8.9±0.9 μM given the affinities of mutant cpFtsY(D283N) for GTP and XTP and the GTP concentration used in this experiment (eq 4 in the Methods). This strongly suggests that the binding of XTP to cpFtsY(D283N) is responsible for the observed inhibitory effect. Taken together, the results in this section show that although cpFtsY(D283N) by itself exhibits a specificity for XTP, this mutant prefers the non-cognate GTP for interacting with and stimulating GTP hydrolysis from cpSRP54. Thus Asp283 and/or the

bound GTP play a much more important role than specifying the nucleotide preference of cpFtsY and likely participate in critical interface interactions with cpSRP54 in the cpSRP54•cpFtsY complex.

Discussion

The chloroplast SRP and SR GTPases are pre-organized to efficiently interact with each other.

cpSRP54 and cpFtsY share 69.5% and 65.4% similarity with their *E. coli* homologues. All the essential motifs in the GTP binding pocket are highly conserved. As expected from the high sequence conservation, both proteins share many biochemical features characteristic of the SRP subfamily of GTPases, including weak nucleotide affinities, fast nucleotide exchange rates, and the ability to reciprocally stimulate each other's GTPase reaction after they form a complex.

Given these similarities, it is surprising that the otherwise universally conserved SRP RNA, which plays a crucial role in eukaryotic and prokaryotic SRP protein targeting pathways, is missing in the chloroplast SRP pathway. In *E. coli*, association between the SRP and SR GTPases is extremely slow, with a rate constant of 5×10^3 $M^{-1}s^{-1}$ (*19*). This slow association rate does not appear to be caused by the extended N-terminal A-domain of *E. coli* FtsY, as truncating the N-terminal 46 amino acids of the A-domain results in identical kinetics of interaction with the SRP GTPase (S.S., unpublished results). Further, *T. aquaticus* FtsY, which lacks an extended N-terminal A-domain, also interacts with its binding partner very slowly in the absence of the SRP RNA (S.S., unpublished results). At this rate and the *in vivo* concentration of these GTPases (nanomolar range), the association between the two GTPases will take hours to complete, whereas protein targeting occurs on the time scale of seconds. One of the important contributions of the SRP RNA is to accelerate complex formation between the two GTPases by 400-fold (*19,*

32). Another contribution of the SRP RNA, albeit minor in comparison, is to increase the rate at which GTP is hydrolyzed from the SRP•SR complex by ~ five–tenfold (*19, 32*). GTP hydrolysis is known to drive disassembly and recycling of the SRP and SR after each round of targeting (*8*). Here, we showed that cpSRP54 and cpFtsY can interact efficiently with each other even in the absence of an SRP RNA: their association rate is at least as fast as that of their *E. coli* homologues that contain the SRP RNA, and GTP hydrolysis from the cpSRP54•cpFtsY complex also occurs at the same rate as the *E. coli* GTPase complex in the presence of the RNA. This helps explain how the chloroplast SRP system can bypass the requirement for the SRP RNA.

Why is the protein–protein interaction so efficient between the chloroplast GTPases? Interaction between the bacterial SRP and SR GTPases is slow presumably due to the requirement for extensive conformational changes during complex formation. One of the important rearrangements is a repositioning of the N-G domain interface, which led to a change of the GTPase site from a floppy, non-specific open state to a closed state in which active site interactions with the bound nucleotide are established (*15*). Thus, one possibility is that cpSRP54 and cpFtsY are pre-organized into the closed conformation that is ready to interact with each other. The results herein strongly suggest that this is the case at least for cpFtsY. Free cpFtsY can specifically recognize its cognate nucleotide, in contrast to *E coli* FtsY which acquires nucleotide specificity only when it forms a complex with SRP. Further, cpFtsY exhibits higher affinities for GTP and GDP than its bacterial homologues, with dissociation constants of 2–3 μM instead of 19–30 μM for *E. coli* FtsY. Finally, the crystal structure of cpFtsY shows that among all the structures of free FtsY from various species, the conformation of apo-cpFtsY is closest to

that observed in the Ffh•FtsY complex, especially with regard to the relative orientation of the N- and G-domains (Chandrasekar et al., manuscript in preparation). These observations strongly support the notion that free cpFtsY is pre-organized in a closed conformation, and thus can interact with cpSRP54 without paying further energetic penalty to rearrange the relative position of the N- and G-domains. It remains to be seen whether cpSRP54 is similarly pre-organized into the closed conformation prior to interaction with cpFtsY.

It appears that the SRP RNA has been evolved to accelerate the very inefficient interaction between the SRP and SR GTPases in classical systems. Although models are abundant (*32*, *37*, *38*), the molecular mechanism by which the SRP RNA acts as a catalyst to accelerate both the formation and disassembly of the SRP•SR complex is still poorly understood. It is possible that in the transition state for complex assembly, the SRP RNA may provide a transient tether that facilitates the rearrangement of one or both GTPases into the closed conformation; alternatively, the RNA and the chloroplast GTPases may employ completely different mechanisms to attain faster association kinetics.

Asymmetic nucleotide hydrolysis from the cpSRP54•cpFtsY complex.

The crystal structure of the *T. aquaticus* Ffh•FtsY complex shows that the two GMPPCP molecules are bound at a composite active site formed at the dimer interface (*12, 13*). Consistent with the composite nature of the active site and the extensive degree of crosstalk between the two GTPase sites, the two nucleotides are hydrolyzed at the same rate from the *E. coli* SRP•FtsY complex. These observations have led to earlier

proposals of concerted GTP hydrolyses in the SRP•SR complex (*20*). In contrast to this notion, we showed here that nucleotide hydrolysis in the cpSRP54•cpFtsY complex can be asymmetric, with the nucleotide hydrolyzing ~ tenfold faster from the cpFtsY than the cpSRP54 active site. This observation argues against a concerted mechanism. Even in the *E. coli* system, mutant GTPases have been identified in which GTP is hydrolyzed much faster from the SRP than the FtsY active site (*39*). Further, when either one of the GTPases is bound with a non-hydrolyzable GTP analogue, it can still activate efficient GTP hydrolysis on its binding partner (unpublished results). Together, these results strongly suggest that hydrolyses of the two GTPs in the SRP•SR complex do not proceed through a concerted mechanism or an ordered pathway (i.e., one GTP must be hydrolyzed first before hydrolysis of the second GTP can occur). Rather, each active site can hydrolyze its bound GTP independently.

Even though the nucleotide is hydrolyzed ~ tenfold slower from cpSRP54 than from cpFtsY(D283N), multiple rounds of XTP hydrolysis from the cpSRP54•cpFtsY(D283N) complex is not blocked and occur as efficiently as single turnover reactions (data not shown). Thus, disassembly of the complex must occur on a faster time scale than the second hydrolysis event, implying that SRP and SR can dissociate from one another even when only one of the nucleotides is hydrolyzed. A similar observation was made for the *E. coli* SRP•SR complex (*39*). Together, the data from the *E. coli* and chloroplast systems suggest that only one GTP hydrolysis event is required to drive disassembly of the SRP•SR complex. It remains to be clarified how many GTPs need to be hydrolyzed during each round of protein targeting, and what the precise role of each GTP hydrolysis event is.

The nucleotide specificity determinant of cpFtsY, Asp283, mediates molecular crosstalk between the two GTPases.

Given the high specificity of cpFtsY(D283N) for XTP, it is surprising to find that this mutant prefers GTP over XTP when it forms a complex with cpSRP54. This strongly suggests that Asp283, in addition to conferring nucleotide specificity to cpFtsY, also contributes to interactions at the dimer interface. The behavior of cpFtsY(D283N) is reminiscent of an XTP-specific mutant of the *E. coli* SRP GTPase, Ffh(D251N), which also prefers the non-cognate GTP over cognate XTP when it forms a complex with FtsY (*31*). The crystal structure confirms that Asp251 makes an important interface contact with Lys390 from FtsY (*12, 13*). A similar interaction could be formed by Asp283 of cpFtsY with a hydrogen bond donor (–AH) at the interface of the cpSRP54•cpFtsY complex (Figure 1.8A). When cpFtsY(D283N) is bound to XTP, mutation of Asp283 to Asn destroys this interface contact and compromises the interaction between the two GTPases (Figure 1.8B). In contrast, replacement of XTP with GTP no longer constrains Asn283 in this particular configuration; a rotation around the C^{β}–C^{γ} bond can reposition the carbonyl oxygen of Asn283 close to the hydrogen bond donor from cpSRP54, thus restoring this interface contact (Figure 1.8C). Alternatively, the exocyclic amino group of GTP could directly interact with a hydrogen bond acceptor from cpSRP54 (–B:, Figure 1.8D), therefore replacement of GTP with XTP compromises the cpSRP54–cpFtsY(D283N) interaction. In either scenario, our results map the G-IV motif of cpFtsY and its bound nucleotide to the dimer interface between the two GTPases, and demonstrate the presence of extensive crosstalk between the two GTPase sites.

Perspective

The results here help rationalize why the chloroplast SRP targeting pathway bypasses the requirement for the SRP RNA, as the SRP and SR GTPases from chloroplast can interact efficiently with one another without the help from the SRP RNA. The novel cpSRP43 protein, which together with cpSRP54 forms the chloroplast SRP, has often been viewed as a functional replacement for the SRP RNA. Our results show that the chloroplast GTPases have evolved to efficiently interact with one another, and no additional acceleration has been observed in the presence of cpSRP43 (Supplementary Figure 1.S2). Therefore, cpSRP43 does not replace all of the functions of the SRP RNA. This novel chloroplast protein may have evolved to mediate other important roles of the SRP RNA in the protein targeting reaction, such as recognition of the cargo protein (*25, 29*). Analogously, the SRP RNA may have been evolved to interact with ribosomal RNAs during co-translational protein targeting in the classical SRP pathways (*40*, *41*).

It is fascinating to speculate on the evolutionary origin of the vast difference in the kinetics of interaction between the SRP and SR GTPases from chloroplast vs. classical SRP pathways, and why cells have evolved the SRP RNA to deal with the inefficient interaction between SRP and SR GTPases during targeting of proteins from the cytosol to membrane compartments. An intriguing possibility is that the slow interaction kinetics between the SRP and SR GTPases in classical pathways allow for additional opportunities for regulation and for improving fidelity. The interaction kinetics between SRP and SR are still relatively slow even with the RNA present; *in vivo*, however, the presence of the ribosome, the cargo protein, or the membrane translocon could further accelerate the interaction between the two GTPases. The SRP RNA, bound

in close vicinity to the signal sequence binding site, could respond to cues such as cargo binding and mediate the additional stimulation of SRP–SR interaction by the cargo. In this way, the SRP RNA could mediate the communication between the cargo binding M-domain and the GTPase domain of SRP, and potentially provide a checkpoint to improve the fidelity of the classical SRP pathway, which needs to sort a vast number of cellular proteins to subcellular compartments. In contrast, a much smaller number of proteins need to be handled by the cpSRP pathway, thus alleviating the need for this regulatory RNA molecule.

Acknowledgment

We thank Dr. R. Henry for the bacterial expression vectors for cpSRP54 and cpFtsY, Dr. J. Campbell and the rest of the Shan lab for comments on the manuscript, and Dr. P. Walter for insightful discussions and intellectual support. S.S. was supported by career awards from the Burroughs Wellcome Fund and the Camile and Henry Dreyfus Foundation, P.J.A. is supported by the Bray fellowship.

Table 1.1 Rate and equilibrium constants for the GTPase cycle of cpSRP54 and cpFtsY[a]

Equilibrium or Rate Constant	Values determined
k_1	3.7×10^6 $M^{-1}s^{-1}$
k_{-1}	10.4 ± 0.8 s^{-1}
K_1	2.8 ± 0.4 μM
k_2	0.017 ± 0.002 min^{-1}
k_3	2.9×10^6 $M^{-1}s^{-1}$
k_{-3}	32 ± 2 s^{-1}
K_3	5.1 ± 0.3 μM
k_1'	2.6×10^6 $M^{-1}s^{-1}$
k_{-1}'	5.4 ± 0.3 s^{-1}
K_1'	2.1 ± 0.2 μM
k_2'	0.0045 ± 0.002 min^{-1}
k_3'	2.6×10^6 $M^{-1}s^{-1}$
k_{-3}'	8.1 ± 0.2 s^{-1}
K_3'	3.1 ± 0.2 μM
k_4	$\geq 8.6 (\pm 0.3) \times 10^5$ $M^{-1}s^{-1}$
k_{-4}	N. D.
k_5	0.83 ± 0.04 s^{-1}
k_6	≥ 0.83 s^{-1}

[a] The rate and equilibrium constants are defined in Figure 1.1. The details and justifications of how each microscopic rate constant is determined from the experimental data are provided in Supplementary Material. N. D., not determined

Table 1.2 Nucleotide affinities of cpSRP54, wild-type cpFtsY, and mutant cpFtsY(D283N)

	K_d (μM)					
Protein	**GTP**	**GDP**	**GppNHp**	**XTP**	**XDP**	**XppNHp**
cpSRP54	2.8[a]/ 6.5[c]	5.1[b] / 11[c]	26[b]	50[b]	N.D.[d]	N.D.[d]
cpFtsY wild-type	2.1[a] /1.9[c]	3.1[c]	4.6[b]	510[b]	557[b]	970[b]
cpFtsY(D283N)	76[b]	180[b]	360[b]	2.2[a] /2.7[c]	6.5[c]	34[b]

[a]Determined by cpFtsY concentration dependences as described in Methods

[b]Determined by inhibition methods as described in Methods

[c]Determined by fluorescence using mant-nucleotides as described in Methods

[d]N.D., not determined

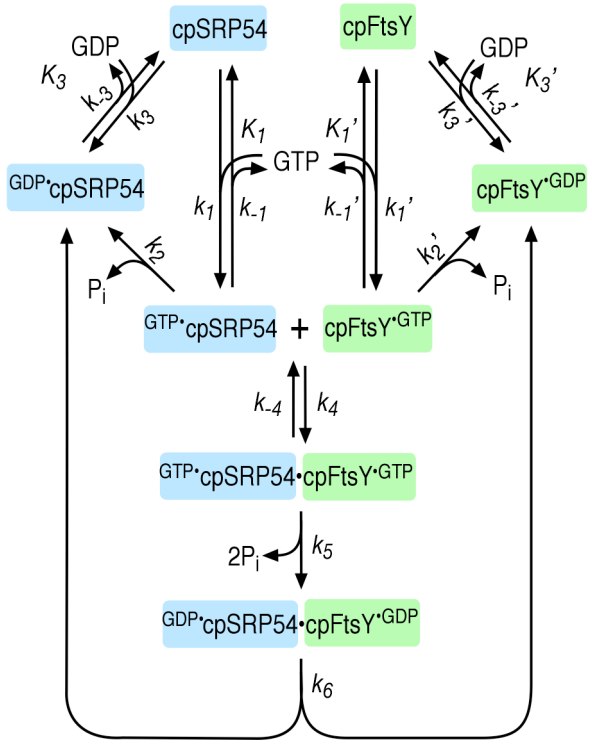

Figure 1.1 Schematic depiction of the GTPase cycles of cpSRP54 (*blue*) and cpFtsY (*green*). Superscripts depict the nucleotide bound to each protein. The triangular cycles on the top left and right depict the basal GTPase cycles of cpSRP54 and cpFtsY, respectively. Binding of GTP to cpSRP54 (or cpFtsY) is characterized by the association rate constant k_1 (or k_1'), dissociation rate constant k_{-1} (or k_{-1}'), and equilibrium dissociation constant K_1 (or K_1'). Rate constants for GTP hydrolysis from cpSRP54 and cpFtsY are denoted by k_2 and k_2', respectively. Binding of GDP to cpSRP54 (or cpFtsY) is characterized by the association rate constant k_3 (or k_3'), dissociation rate constant k_{-3} (or k_{-3}'), and equilibrium dissociation constant K_3 (or K_3'). Complex formation between cpSRP54 and cpFtsY is characterized by the association rate constant k_4 and dissociation rate constant k_{-4}. The two bound GTPs are hydrolyzed from the ^{GTP}•cpSRP54•cpFtsY$^{•GTP}$ complex, represented collectively by the rate constant k_5. The ^{GDP}•cpSRP54•cpFtsY$^{•GDP}$ complex then dissociates with a rate constant k_6.

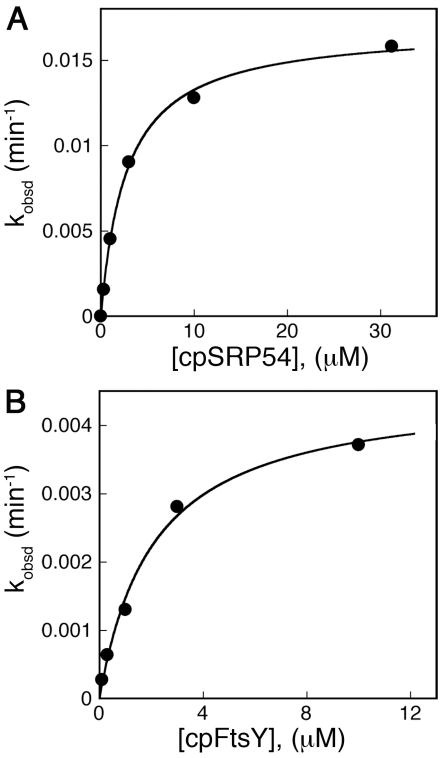

Figure 1.2 Basal GTPase reactions of cpSRP54 (A) and cpFtsY (B). The data were fit to eq 1 in Methods and gave a k_{max} of 0.017 min^{-1} and $K_{1/2}$ of 2.8 μM for cpSRP54, and a k_{max} of 0.0045 min^{-1} and $K_{1/2}$ of 2.1 μM for cpFtsY.

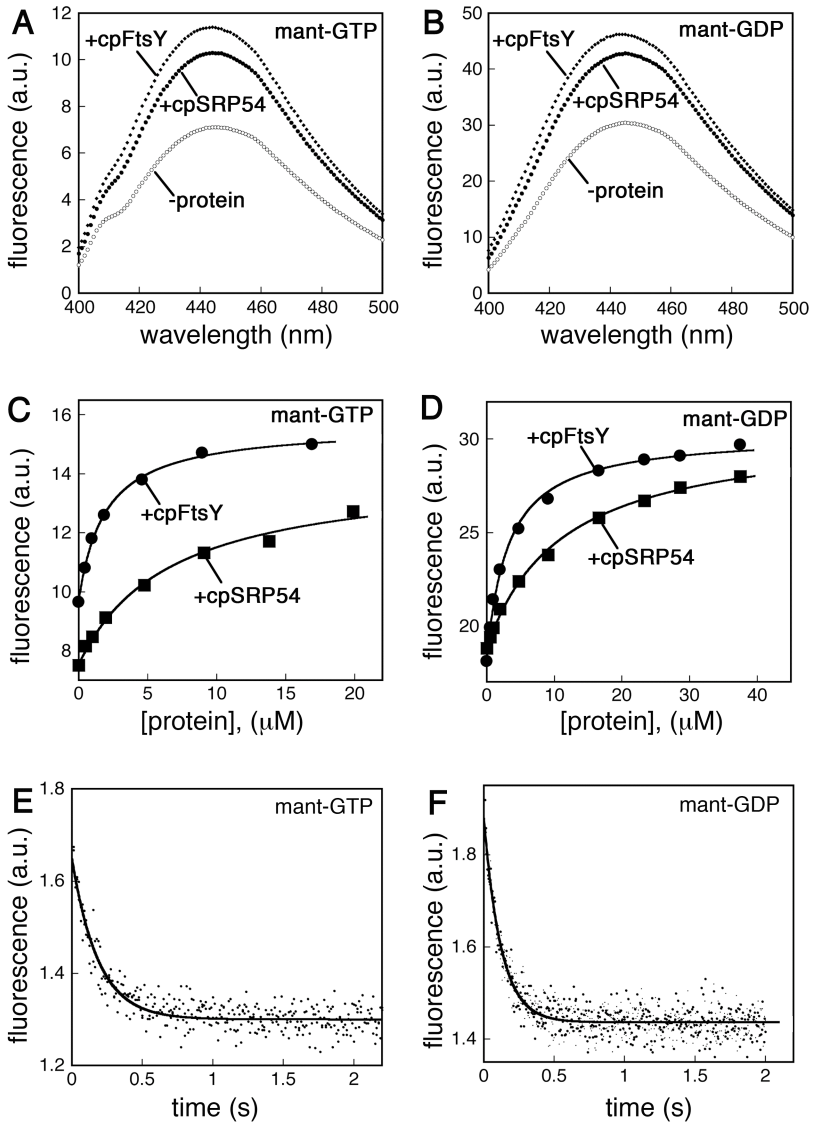

Figure 1.3 Interaction of nucleotides with cpSRP54 and cpFtsY. (A–B) Fluorescence emission spectra of mant-GTP (A) or mant-GDP (B) in the absence of protein (○) and in the presence of 5 μM cpSRP54 (●) or cpFtsY(◆). (C–D) Titration of the fluorescence changes of mant-GTP (C) and mant-GDP (C) in the presence of of cpSRP54 (■) or cpFtsY (●). The data were fit to eq 5 in Methods and the K_d values are summarized in Table 1.2. (E–F) Dissociation of mant-GTP (E) and mant-GDP (F) from cpFtsY. The data were fit to single exponential rate equations and gave dissociation rate constants of 5.4 and 8.1 s^{-1} for mant-GTP and mant-GDP, respectively.

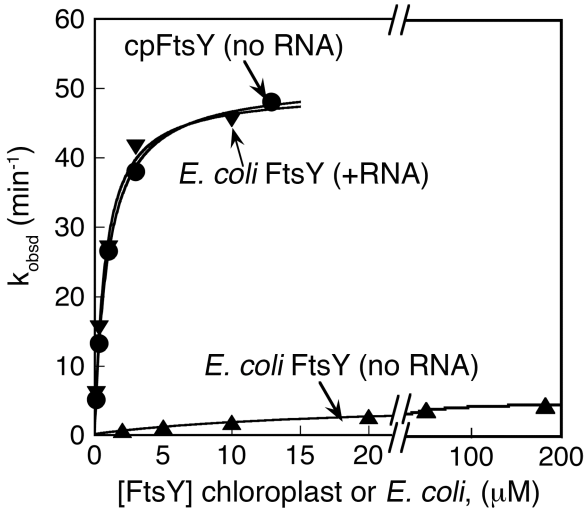

Figure 1.4 Interaction of cpSRP54 and cpFtsY is much more efficient than that of their *E. coli* homologues. Rates of the stimulated GTPase reaction were determined for cpSRP54 (100 nM) and cpFtsY (●), or for *E. coli* Ffh (100 nM) and *E. coli* FtsY with (▼) and without 4.5S SRP RNA (▲). The data were fit to eq 2 in the Methods, and gave a k_{cat} value of 50 min^{-1} and a K_m value of 0.97 μM for the chloroplast GTPases, and k_{cat} values of 49 and 4.8 min^{-1} and K_m values of 0.76 and 18 μM for the *E. coli* GTPases with and without the SRP RNA, respectively.

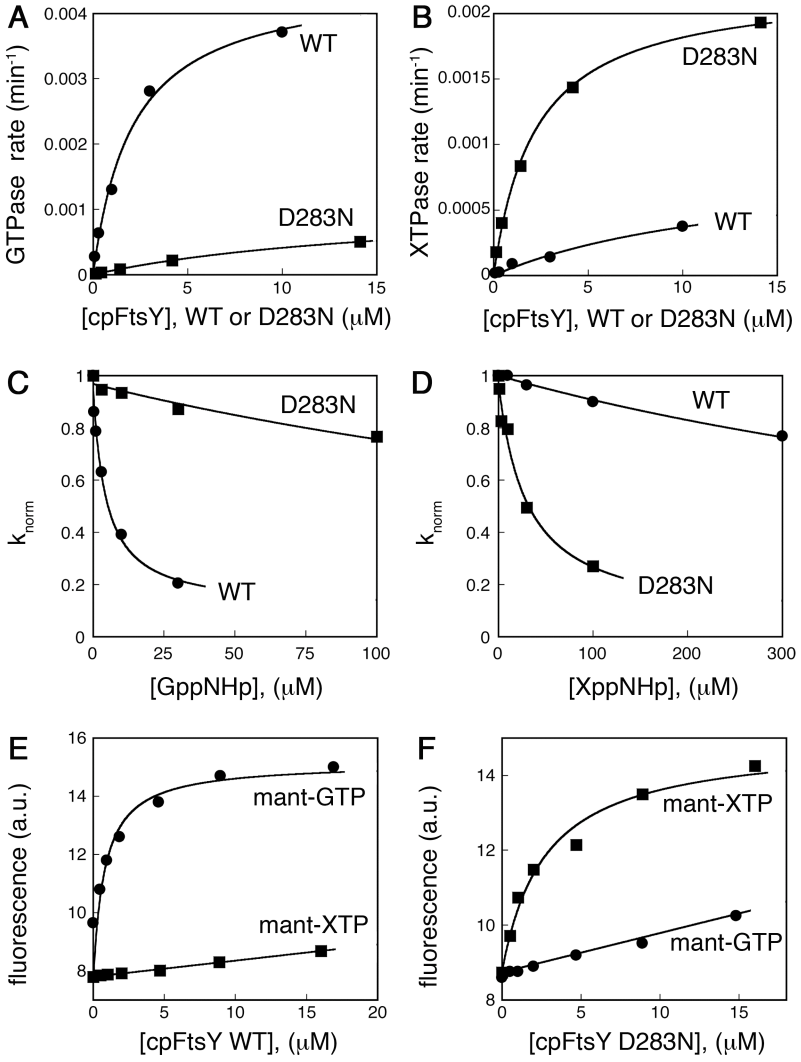

Figure 1.5 cpFtsY preferentially binds and hydrolyzes its cognate nucleotide. (A–B) Basal GTPase (A) and XTPase (B) reactions of wild-type cpFtsY (●) and mutant cpFtsY(D283N) (■). The data were fit to eq 1 and gave a k_{max} value of 0.0045 min^{-1} and a $K_{1/2}$ value of 2.1 μM for GTP hydrolysis by wild-type cpFtsY, and a k_{max} value of 0.0022 min^{-1} and a $K_{1/2}$ value of 2.2 μM for XTP hydrolysis by mutant cpFtsY(D283N). (C) GppNHp binds more strongly to wild-type cpFtsY (●) than to mutant cpFtsY(D283N) (■). (D) XppNHp binds more strongly to mutant cpFtsY(D283N) (■) than to wild-type cpFtsY (●). The K_i values are reported in Table 1.2. (E–F) Titration of the change in fluorescence of mant-GTP (●) and mant-XTP (■) upon binding to wild-type cpFtsY (E) and mutant cpFtsY(D283N) (F). The data were fit to eq 5 and the K_d values are summarized in Table 1.2.

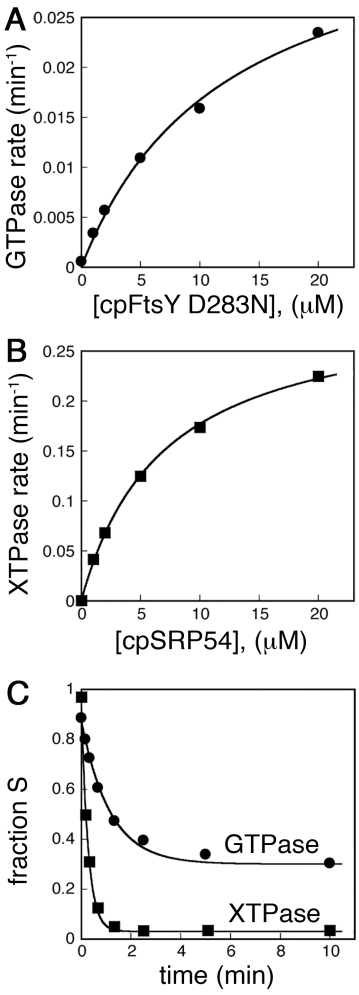

Figure 1.6 Nucleotide hydrolyses from the cpSRP54•cpFtsY(D283N) complex are asymmetric. (A) Stimulation of the GTPase reaction of cpSRP54 by cpFtsY(D283N), determined as described in Methods using 0.2 μM cpSRP54 and 20 μM XTP. The data were fit to eq 1 and gave a maximal rate constant of 0.037 min^{-1}. (B) Stimulation of the XTPase reaction of cpFtsY(D283N) by cpSRP54, determined as described in Methods using 0.2 μM cpFtsY(D283N) and 20 μM GTP. The data were fit to eq 1 and gave a maximal rate constant of 0.30 min^{-1}. (C) Time courses for GTP and XTP hydrolyses from the ^{GTP}•cpSRP54•cpFtsY(D283N)•^{XTP} complex, determined as described in Methods. The data were fit to single-exponential rate equations and gave rate constants of 0.86 and 3.7 min^{-1} for the GTPase reaction (●) and XTPase reactions (■), respectively.

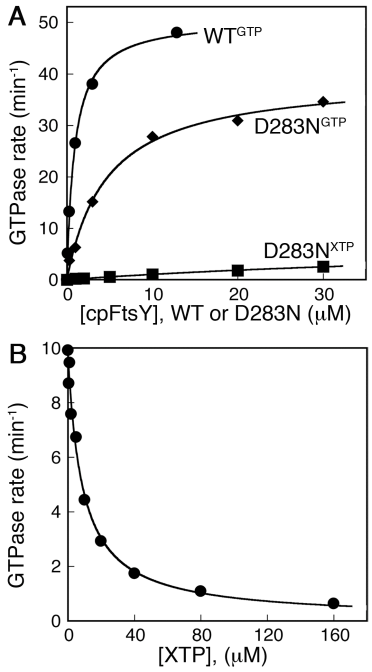

Figure 1.7 cpFtsY(D283N) prefers GTP over XTP when it forms a complex with cpSRP54. (A) GTP hydrolysis rates when cpSRP54 (100–500 nM) interacts with wild-type cpFtsY (●), cpFtsY(D283N) bound to GTP (◆) and cpFtsY(D283N) bound to XTP (■). The following nucleotide concentrations were used: 100 μM GTP for reaction with wild-type cpFtsY, 200 μM GTP for reaction with cpFtsY(D283N) bound to GTP, and 20 μM GTP and 50 μM XTP for reaction with cpFtsY(D283N) bound to XTP. The data were fit to eq 2, which gave k_{cat} values of 50 (●) and 39 min^{-1} (◆). (B) XTP inhibits the ability of GTP-bound cpFtsY(D283N) to stimulate GTP hydrolysis by cpSRP54. Reactions were carried out in the presence of 500 nM cpSRP54, 2 mM cpFtsY(D283N), and 200 μM GTP, as described in the Methods. The data were fit to eq 3 and gave an apparent inhibition constant of 9.0 μM.

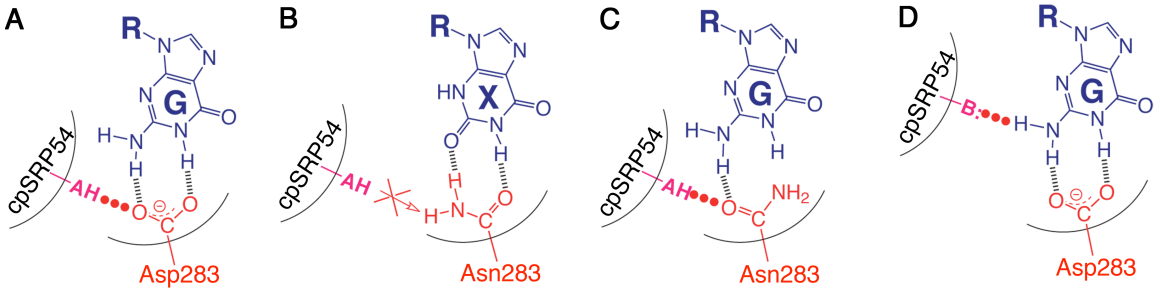

Figure 1.8 Model for the interactions of cpSRP54 with the side chain of cpFtsY Asp283 or with GTP. (A–C) Proposed interactions between the side chain of residue 283 with a hydrogen bond donor from cpSRP54 (–AH) for the wild-type cpSRP54•cpFtsY complex (A) and the cpSRP54•cpFtsY(D283N) complex with XTP (B) or GTP (C) bound to cpFtsY(D283N). (D) The GTP bound to cpFtsY interacts with a hydrogen bond acceptor (–B:) from cpSRP54.

Supplementary Materials

Determination of the microscopic rate constants:

Basal GTP binding and hydrolysis (K_1, k_2 and K_1', k_2'). The chemical step is rate-limiting for the basal GTPase reaction of cpSRP54, as the maximal rate constant of GTP hydrolysis (0.017 min^{-1}; Figure 1.2A) is 4×10^4 -fold slower than the rate at which GTP dissociates from the enzyme active site (10.4 s^{-1}; Figure 1.3E), Therefore, the $K_{1/2}$ value obtained from the data in Figure 1.2A is equal to K_1, the equilibrium dissociation constant for GTP, and the k_{max} value from the same figure is equal to k_2, the rate constant for GTP hydrolysis from the $^{GTP\bullet}$cpSRP54 complex. For the same reason, the chemical step is rate-limiting for the basal GTPase reaction of cpFtsY. Therefore, the $K_{1/2}$ value obtained from the data in Figure 1.2B is equal to K_1', the dissociation constant for GTP, and the k_{max} value obtained from the same figure is equal to k_2', the rate constant for GTP hydrolysis from the cpFtsY$^{\bullet GTP}$ complex. The values of K_1 and K_1' were also determined independently by fluorescence assays (Figure 1.3C) as described in the text.

GDP binding to cpSRP54 and cpFtsY (K_3 and *K_3').* The binding affinities of GDP for both proteins were determined by using GDP as a competitive inhibitor of the basal GTPase reaction, as described previously, and by fluorescence assays (Figure 1.3D) as described in the text.

Nucleotide dissociation rate constants (k_{-1}, k_{-1}' and k_{-3}, k_{-3}'). The rate constants for nucleotide dissociation from each protein were measured using fluorescent mant-GTP and mant-GDP in pulse-chase experiments (Figure 1.3E and 1.3F and data not shown) as described in the text.

Nucleotide association rate constants (k_1, k_1' and k_3, k_3'). The rate constants for binding of GTP and GDP to both proteins were obtained from the equilibrium dissociation constant and the dissociation rate constant for each nucleotide, determined as described above, using $k_{on} = k_{off} / K_d$.

Rate constant for complex formation (k_4). The association rate constant between cpSRP54 and cpFtsY was not determined directly due to the lack of a direct protein–protein binding assay, and was estimated from the value of k_{cat}/K_m for the stimulated GTPase reaction; this value provides a lower limit for k_4, as explained in the Results section.

Rate constant for GTP hydrolysis in the $^{GTP\bullet}$cpSRP54•cpFtsY$^{\bullet GTP}$ complex (k_5). This rate constant was derived from the value of k_{cat} determined from the stimulated GTPase reaction between cpSRP54 and cpFtsY (Figure 1.4, circles). Several observations suggest that product release is not rate-limiting for k_{cat}. First, the value of k_{cat} is the same, within experimental error, as the rate constant of GTP hydrolysis from the $^{GTP\bullet}$cpSRP54•cpFtsY$^{\bullet GTP}$ complex determined under single turnover conditions (data not shown). Second, the time course for the reaction: $^{GTP\bullet}$cpSRP54•cpFtsY$^{\bullet GTP}$ → products is consistent with a single exponential rate without exhibiting a burst phase (Supplementary Figure 1.S1). Thus, steps prior to GTP hydrolysis, rather than product release, is rate-limiting for the stimulated GTPase reaction from the $^{GTP\bullet}$cpSRP54•cpFtsY$^{\bullet GTP}$ complex. Therefore, k_{cat} represents the sum of rate constants for hydrolysis of the two GTPs from the $^{GTP\bullet}$cpSRP54•cpFtsY$^{\bullet GTP}$ complex (k_5) and may

be limited by either the chemical step itself, or a conformational change prior to GTP hydrolysis.

Rate constant for complex dissociation (k_6). For the same reasons stated in the previous paragraph, the value of k_{cat} sets a lower limit for the rate of product release (k_6), which has not been directly measured in this study.

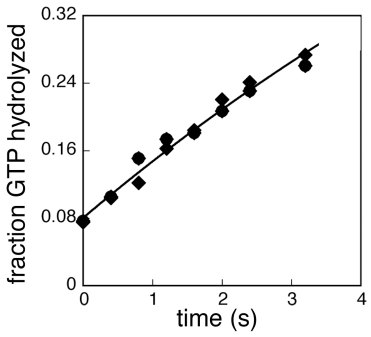

Supplementary Figure 1.S1 The time course for GTP hydrolysis from the cpSRP54•cpFtsY complex shows no obvious burst phase. The reaction was carried out in the presence of 12.5 μM cpSRP54, 15 μM cpFtsY, and 100 μM GTP doped with trace amounts of GTP*; the high concentration of protein relative to GTP is used to maximize the chance of observing the presence of a burst phase. The different symbols represent data from two independent measurements. The line is a fit of the initial part of the time course to a single-exponential rate equation.

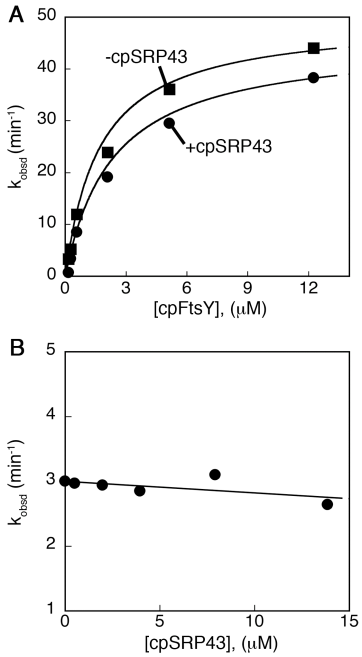

Supplementary Figure 1.S2 cpSRP43 shows no significant effect on GTPase activity of cpSRP54 and cpFtsY. (A) Rates of the stimulated GTPase reactions were determined for cpSRP54 (100 nM) and increasing concentration of cpFtsY in the presence of 100 μM GTP. In the presence (●) of 1 μM cpSRP43, the fit of the data to eq 2 in the Methods gave a k_{cat} value of 49.5 min^{-1} and a K_m value of 1.7 μM. In the absence (■) of cpSRP43, a k_{cat} value was 45.5 min^{-1} and a K_m value was 2.3 μM. (B) Rates of the stimulated GTPase reactions were determined for cpSRP54•cpFtsY complex (100 nM) in the presence of increasing concentration of cpSRP43. No significant stimulation or inhibition was observed compared to the reaction rate in the absence of cpSRP43.

References:

1. Keenan, R. J., Freymann, D. M., Stroud, R. M., and Walter, P. (2001) The signal recognition particle, *Annu. Rev. Biochem. 70*, 755–775.
2. Walter, P., and Johnson, A. E. (1994) Signal sequence recognition and protein targeting to the endoplasmic reticulum membrane, *Ann. Rev. Cell Biol. 10*, 87–119.
3. Walter, P., Ibrahimi, I., and Blobel, G. (1981) Translocation of proteins across the endoplasmic reticulum I. Signal Recognition Protein (SRP) binds to *in vitro* assembled polysomes synthesizing secretory protein, *J. Cell. Biol. 91*, 545–550.
4. Gilmore, R., Blobel, G., and Walter, P. (1982a) Protein translocation across the endoplasmic reticulum: 1. Detection in the microsomal membrane of a receptor for the signal recognition particle, *J. Cell Biol. 95*, 463–469.
5. Gilmore, R., Walter, P., Blobel, G. (1982b) Protein translocation across the endoplasmic reticulum. II. Isolation and characterization of the signal recognition particle receptor, *J. Cell Biol. 95*, 470–477.
6. Gorlich, D., Prehn, S., Hartmann, E., Kalies, K. U., and Rapoport, T. A. (1992) §A mammalian homolog of Sec61p and SecYp is associated with ribosomes and nascent polypeptides during translocation, *Cell 71*, 489–503.
7. Simon, S. M., and Blobel, G. (1991) A protein-conducting channel in the endoplasmic reticulum, *Cell 65*, 371–380.
8. Connolly, T., Rapiejko, P. J., Gilmore, R. (1991) Requirement of GTP hydrolysis for dissociation of the signal recognition particle from its receptor, *Science 252*, 1171–1173.
9. Freymann, D. M., Keenan, R. J., Stroud, R. M., and Walter, P. (1997) Structure of the conserved GTPase domain of the signal recognition particle, *Nature 385*, 361–364.
10. Montoya, G., Svensson, C., Luirink, J., and Sinning, I. (1997) Crystal structure of the NG domain from the signal recognition particle receptor FtsY, *Nature 385*, 365–368.
11. Reyes, C. L., Rutenber, E., Walter, P., and Stroud, R.M. (2007) X-ray structures of the signal recognition particle receptor reveal targeting cycle intermediates, *PLoS ONE 2*, e607.
12. Egea, P. F., Shan, S., Napetschnig, J., Savage, D.F., Walter, P., and Stroud, R.M. (2004) Substrate twinning activates the signal recognition particle and its receptor, *Nature 427*, 215–221.
13. Focia, P. J., Shepotinovskaya, I.V., Seidler, J.A., and Freymann, D.M. (2004) Heterodimeric GTPase Core of the SRP Targeting Complex, *Science 303*, 373–377.
14. Lu, Y., Qi, H.-Y., Hyndman, J. B., Ulbrandt, N. D., Teplyakov, A., Tomasevic, N., and Bernstein, H. D. (2001) Evidence for a novel GTPase priming step in the SRP protein targeting pathway, *EMBO J. 20*, 6724–6734.
15. Shan, S., and Walter, P. (2003) Induced Nucleotide Specificity in a GTPase, *Proc. Natl. Acad. Sci. U.S.A. 100*, 4480–4485.

16. Jagath, J. R., Rodnina, M. V., Lentzen, G., and Wintermeyer, W. (1998) Interaction of guanine nucleotides with the signal recognition particle from *Escherichia coli*, *Biochemistry 37*, 15408–15413.
17. Jagath, J. R., Rodnina, M. V., and Wintermeyer, W. (2000) Conformational changes in the bacterial SRP receptor FtsY upon binding of guanine nucleotides and SRP, *J. Mol. Biol. 295*, 745–753.
18. Moser, C., Mol, O., Goody, R. S., and Sinning, I. (1997) The signal recognition particle receptor of *Escherichia coli* (FTsY) has a nucleotide exchange factor built into the GTPase domain, *Proc. Natl. Acad. Sci. U. S. A. 94*, 11339–11344.
19. Peluso, P., Shan, S., Nock, S., Herschlag, D., and Walter, P. (2001) Role of SRP RNA in the GTPase cycles of Ffh and FtsY, *Biochemistry 40*, 15224–15233.
20. Powers, T., and Walter, P. (1995) Reciprocal stimulation of GTP hydrolysis by two directly interacting GTPases, *Science 269*, 1422–1424.
21. Walter, P. and Blobel, G. (1982) Signal recognition particle contains a 7S RNA essential for protein translocation across the endoplasmic reticulum, *Nature 299*, 691–698.
22. Walter, P. and Blobel, G. (1983) Disassembly and reconstitution of signal recognition particle, *Cell 34*, 525–533.
23. Poritz, M. A., Strub, K., and Walter, P. (1988) Human SRP RNA and *E. coli.* 4.5S RNA contain a highly homologous structural domain, *Cell 55*, 4–6.
24. Struck, C. R. J., Toschka, H. Y., Specht, T., Erdmann, V. A. (1988) Common structural features between eukaryotic 7SL RNAs, eubacterial 4.5S RNA and scRNA and archaebacterial 7S RNA, *Nuc. Acids Res. 16*, 7740–7746.
25. Schuenemann, D., Gupta, S., Persello-Cartieaux, F., Klimyuk, V. I., Jones, J. D. G., Nussaume, L., and Hoffman, N. E. (1998) A novel signal recognition particle targets light-harvesting proteins to the thylakoid membranes, *Proc. Natl. Acad. Sci. USA 95*, 10312–10316.
26. Franklin, K. E., and Hoffman, N. E. (1993) Characterization of a chloroplast homologue of the 54-kDa subunit of the signal recognition particle, *J. Biol. Chem. 268*, 22175–22180.
27. Li, X., Henry, R., Yuan, J., Cline, K., and Hoffman, N.E. (1995) A chloroplast homologue of the signal recognition particle subunit SRP54 is involved in the posttranslational integration of a protein into thylakoid membranes, *Proc. Natl. Acad. Sci. USA 92*, 3789–3793.
28. Tu, C.-J., Schuenemann, D., and Hoffman, N. E. (1999) Chloroplast FtsY, Chloroplast Signal Recognition Particle, and GTP are required to reconstitute the soluble phase of light-harvesting chlorophyll protein transport into thylakoid membranes, *J. Biol. Chem. 274*, 27219–27224.
29. Tu, C. J., Peterson, E. C., Henry, R., and Hoffman, N. E. (2000) The L18 domain of light-harvesting chlorophyll proteins binds to chloroplast signal recognition particle 43, *J. Biol. Chem. 275*, 13187–13190.
30. Yuan, J., Kight, A., Goforth, R.L., Moore, M., Peterson, E.C., Sakons, J., and Henry, R. (2002) ATP stimulates signal recognition particle (SRP)/FtsY-supported protein integration in chloroplasts, *J. Biol. Chem. 277*, 32400–32404.

31. Shan, S., and Walter, P. (2005) Molecular crosstalk between the nucleotide specificity determinant of the SRP GTPases and the SRP receptor, *Biochemistry 44*, 6214–6222.
32. Peluso, P., Herschlag, D., Nock, S., Freymann, D. M., Johnson, A. E., and Walter, P. (2000) Role of 4.5S RNA in assembly of the bacterial signal recognition particle with its receptor, *Science 288*, 1640–1643.
33. Bishop, A., Buzko, O., Heyeck-Dumas, S., Jung, I., Kraybill, B., Liu, Y., Shah, K., Ulrich, S., Witucki, L., Yang, F., Zhang, C., and Shokat, K. M. (2000) Unnatural Ligands for engineered proteins: new tools for chemical genetics, *Annu. Rev. Biophys. Biomol. Struct. 29*, 577–606.
34. Hwang, Y. W., and Miller, D. L. (1987) A mutation that alters the nucleotide specificity of elongation factor Tu, a GTP regulatory protein, *J. Biol. Chem. 262*, 13081–13085.
35. Weijland, A., Parlato, G., and Parmeggiani, A. (1994) Elongation factor Tu D138N, a mutant with modified substrate specificity, as a tool to study energy consumption in protein biosynthesis, *Biochemistry 33*, 10711–10717.
36. Zhong, X.-M., Chen-Hwang, M.-C., Hwang, Y. W. (1995) Switching nucleotide specificity of Ha-Ras p21 by a single amino acid substitution at aspartate 119, *J. Biol. Chem. 270*, 10002–10007.
37. Spanggord, R. J., Siu, F., Ke, A., and Doudna J.A. (2005) RNA-mediated interaction between the peptide-binding and GTPase domains of the signal recognition particle, *Nat. Struct. Mol. Biol. 12*, 1116–1122.
38. Buskiewicz, I., Kubarenko, A., Peske, F., Rodnina, M.V., and Wintermeyer, W. (2005) Domain rearrangement of SRP protein Ffh upon binding 4.5S RNA and the SRP receptor FtsY, *RNA 11*, 947–957.
39. Shan, S., Stroud, R., Walter, P. (2004) Mechanism of association and reciprocal activation of two GTPases, *PLoS Biology 2*, e320.
40. Halic, M., Blau, M., Becker, T., Mielke, T., Pool, M.R., Wild, K., Sinning, I., and Beckmann, R. (2006) Following the signal sequence from ribosomal tunnel exit to signal recognition particle, *Nature 444* 507–511.
41. Schaffitzel, C., Oswald, M., Berger, I., Ishikawa, T., Abrahams, J.P., Koerten, H.K., Koning, R.I., and Ban, N. (2006) Structure of the E. coli signal recognition particle bound to a translating ribosome, *Nature 444*, 503–506.